Structural insights into the catalytic mechanisms of plastic-degrading enzymes

Christos Kosinas[1], Panagiota Karamba[1], Kostas Makryniotis[2], Efstratios Nikolaivits[2], Evangelos Topakas[2], Maria Dimarogona[1]

[1]Department of Chemical Engineering, University of Patras, Patras, Greece
[2]School of Chemical Engineering, National Technical University of Athens, Athens, Greece

An engineered **leaf-branch compost cutinase** (LCC^{ICCG}) (Tournier et al., 2020) and a **glucuronoyl esterase** from *Sporotrichum thermophile* (*St*GE) (Taxeidis et al., 2024) pose as two promising biocatalysts towards poly(ethylene terephthalate)-PET and poly(lactic acid)-PLA degradation. While LCC^{ICCG} is strictly active on PET, StGE displays broader substrate promisquity, being able to tackle PET as well as amorphous PLA polymers. Flexible docking simulations performed with Auto-Dock VINA using PET and PLA oligomers provide **structural insights into this selectivity**, highlighting key **residues that may influence catalytic efficiency or alter substrate specificity**. Such findings could be used for engineering enzymes with enhanced activity toward non-natural polymeric substrates.

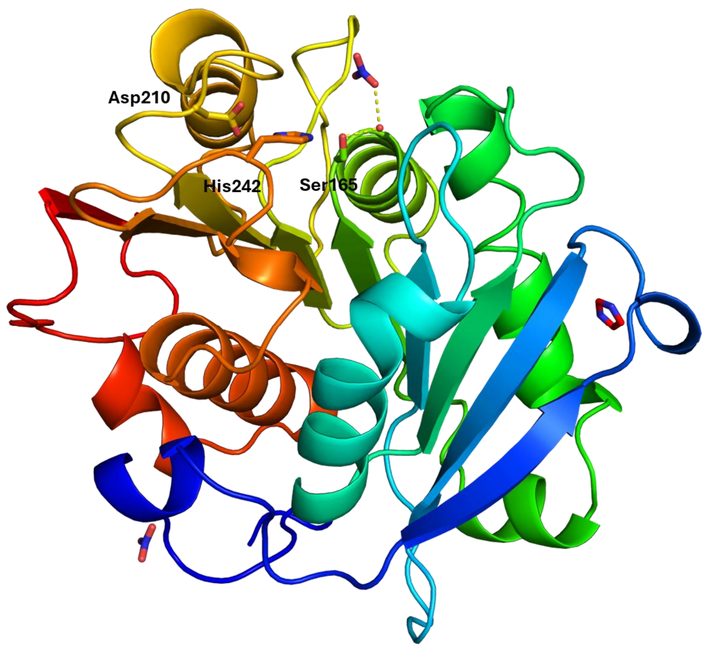

Figure 1: Cartoon representation of LCC^{ICCG} refined at 1.64 Å. Ser165, Asp210 and His242 that constitute the enzyme's active site are shown as sticks. A nitrate molecule originating from the crystallization buffer was modelled inside the active site cavity.

LCC^{ICCG} binds PET oligomers

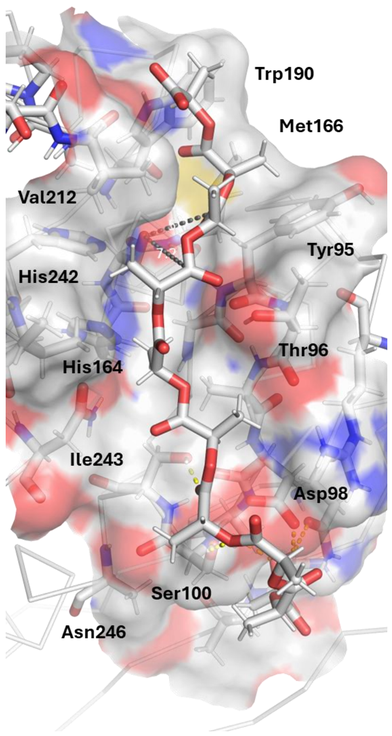

Figure 2: Representation of PLA10 interaction with LCC^{ICCG}

subsite -1	**Ile243, Asn246, Ser101, His164**
subsite +1	**His242, Val212, Ser165, Tyr95, Trp190, Met166, Thr96**
subsite +2	**Gly127, Trp190, Thr192, Pro128, Asp129, Tyr95**

Ligand	Binding Energy (kcal/mol)	Kd (mM)	OG-C (Å)
BHET	5.87	0.049	3.8
2-HE$(MHET)_2$	4.82	0.291	3.9
2-HE$(MHET)_3$	6.57	0.015	3.6
PLA10	6.14	0.031	5.7

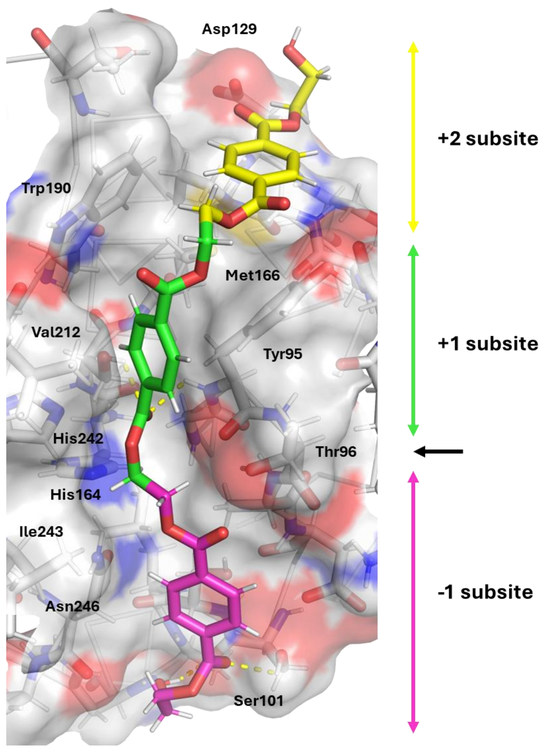

Figure 3: Representation of 2-HE$(MHET)_3$ interaction with LCC^{ICCG}

Evaluation of docking results

- **The C1 atom of carboxyl group should be within 4 Å of the OG atom of the catalytic serine (Yang Y. *et al.*, 2022. Erickson E. *et al.*, 2022).**
- **Selection of results showing the strongest binding (highest binding energy) and lowest estimated dissociation constant (K_d).**

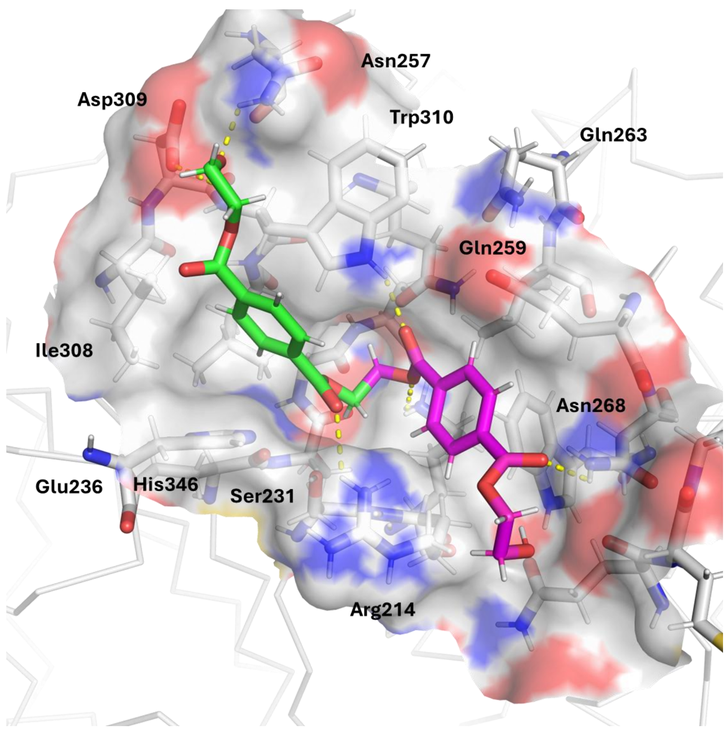

Figure 4: Representation of 2-HE$(MHET)_2$ interaction with *St*GE.

Ligand	Binding Energy (kcal/mol)	Kd (mM)	OG-C (Å)
BHET	4.90	0.257	3.8
2-HE$(MHET)_2$	5.49	0.094	3.6

Binding sites of PLA and PET oligomers on *St*GE

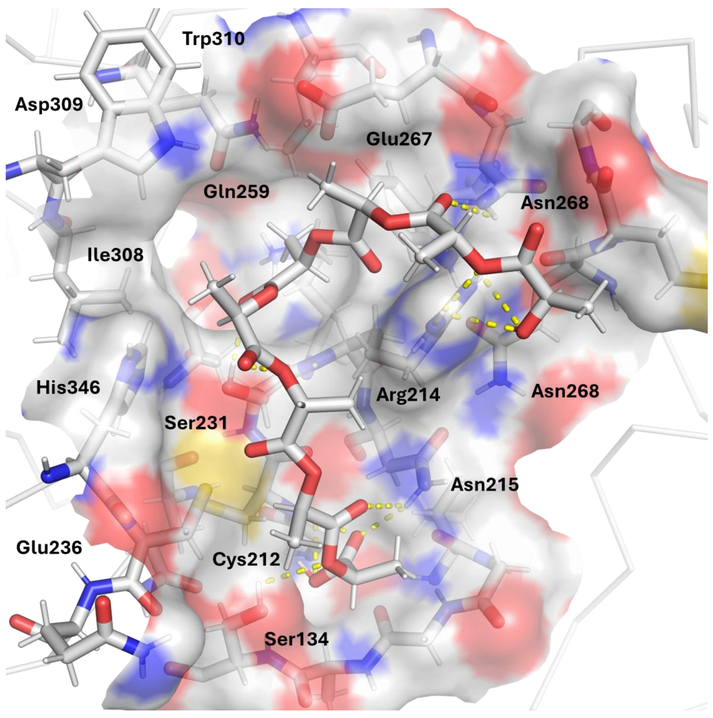

Figure 5: Representation of PLA8 interaction with *St*GE.

Ligand	Binding Energy (kcal/mol)	Kd (mM)	OG-C (Å)
4PLA	5.65	0.072	3.6
6PLA	6.65	0.013	3.8
8PLA	7.37	0.004	3.7
10PLA	6.11	0.033	3.5

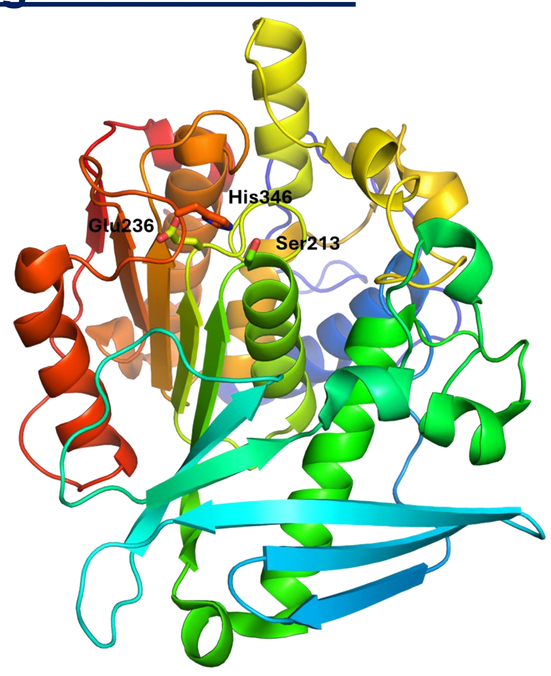

Figure 6: Cartoon representation of *St*GE refined at 1.55 Å. Ser213, His346 and Glu236 that constitute the enzyme's active site are shown as sticks.

Conclusions

LCC^{ICCG}

- Residues of LCC^{ICCG} forming the binding site that accommodates 2-HE$(MHET)_3$ are identified.
- **Several hydrophobic residues of LCC^{ICCG} (Ile243, Tyr95 and Trp190) mediate critical hydrophobic and pi-pi interactions with PET's phenolic moieties.**
- **Trp190, Met168 and Tyr95** cannot accommodate the methyl group of PLA. Mutations could unlock PLA activity.

*St*GE

- 2-HE$(MHET)_2$ subsites are identified. Hydrophobic contacts and hydrogen bonds stabilize MHET units.
- A conformational shift of Arg214 near the catalytic serine may stabilize the substrate and thus facilitate the nucleophile attack of serine on the carboxyl carbon.
- On the contrary, during PLA binding, Arg241 adopts an alternative conformation. **Arg214 multiple conformations reshape the binding pocket, providing a structural basis for the enzyme's substrate promiscuity**.

References

[4] Taxeidis, G. *et al,* (2024). *ACS Sustain Chem Eng* **12**, 5943–5952.
[5] Tournier, V. *et al*., (2020). *Nature* **580**, 216–219.
[3] Yang Y. *et al*., (2022). *Nature Communications* **14**: 1645
[4] Erickson, E. *et al*., (2022). *Nature Communications* **13**:7850

Acknowledgements

This research is supported by the Basic Research Financing (Horizontal support for all Sciences), National Recovery and Resilience Plan (Greece 2.0) Action, under the "Sub-action II Funding Projects in Leading-Edge Sectors" (EnZyReMix, project number: 15024). We would like to thank the MAX IV Laboratory for beamtime on the BioMAX beamline under proposal 20240403.